ELSEVIER

Journal of Atmospheric and Solar-Terrestrial Physics 70 (2008) 1110–1121

Journal of ATMOSPHERIC AND SOLAR-TERRESTRIAL PHYSICS

www.elsevier.com/locate/jastp

# Assessing the state of the atmospheric acoustic channel using the IDEAS data on long-distance microbarom propagation

A.G. Sorokin*, E.A. Ponomarev

*Institute of Solar-Terrestrial Physics, Siberian Branch, Russian Academy of Sciences, P.O. Box 291, Irkutsk 664033, Russian Federation*

Received 13 July 2007; received in revised form 11 January 2008; accepted 27 January 2008
Available online 6 February 2008

**Abstract**

This paper discusses the technique for assessing the state of atmospheric acoustic channels (AACs) for the long-distance propagation of microbaroms. We calculated two possible microbarom propagation paths to station "Badary" from the sources located in (1) the North Atlantic at an azimuth of 320° and (2) the Northwestern Pacific at an azimuth of 60°. We investigate the spatio-temporal structure of the AAC. The experimental data are compared with modeling results.


*Keywords:* Atmospheric acoustic channel; Atmospheric model; Infrasound station; Long-distance propagation; Microbaroms; Number of modes

## 1. Introduction

Identification of infrasound signals from remote sources is rooted in research into the propagation of sound from volcanic eruptions in Japan in the early 20th century. Evidence provided by event witnesses was used as information on the propagation of a sound signal. Those pioneering studies revealed an asymmetry in the propagation of acoustic signals, and in the 1920s the existence of distance-alternating audibility and acoustic shadow zones was ascertained, and the main regularities of sound wave reflection in the atmosphere were established (Massey and Boyd, 1957, 1962). To date, we know a great deal about the atmospheric structure and about the existence of atmospheric acoustic channels (AACs). However, knowledge of "average" data is insufficient because of the high spatial and temporal variability of such atmospheric parameters as temperature, and wind direction and velocity. Heterogeneous information on atmospheric parameters obtained in different places and by different methods is generalized by means of high integration of evidence (the ordered accumulation of data in a uniform format), which was obtained through aerological sounding and from satellite and ground-based measurements, as well as by numerical simulations. Such an approach is generally used in constructing models to provide information on the distribution of atmospheric parameters for a given space–time interval. An MSIS 2000-based generalized ground to space (G2S) model of the atmosphere is currently under development in the USA (Drob, 2003; Gibson and Drob, 2005; Drob et al., 2003), which provides a reasonably good agreement with instantaneous measurements of

*Corresponding author. Tel.: +7 3952 424491; fax: +7 3952 425557.
*E-mail addresses:* sor@iszf.irk.ru (A.G. Sorokin), pon@iszf.irk.ru (E.A. Ponomarev).

1364-6826/$ - see front matter © 2008 Elsevier Ltd. All rights reserved.
doi:10.1016/j.jastp.2008.01.011

atmospheric parameters. Still, this model does not afford the inclusion of many atmospheric parameters in the formation of the ACC, such as the effects of an atmospheric cyclone or a sudden stratospheric warming. Some progress along these lines can be expected through the use of the meteorological data archived in the IDEAS (Investigation of Distributed Environmental Archives System, USA) system, a network distributed software system, and one of the IDEAS sites is located in Russia (Zhizhin and Andreyev, 2004).

## 2. The principles of construction of the acoustic path

Acoustic processes are of great importance in the physics of the atmosphere by providing the transfer of energy, both along the spectrum and in space. Therefore, the acoustic facilities are an important element of atmospheric monitoring instrumentation as well as provides a basis for remote monitoring of the production and military activities. Also, an important element of the control and monitoring systems is provided by the model of the acoustic channel that makes it possible to assess accessibility or inaccessibility of the signal source depending on its location and the meteorological situation. The implications of this problem for basic and applied research are such that many large research teams (in the USA, France, the Netherlands, Sweden, and India) are engaged in these issues (Blanc, 2001; Liszka, 1974). There are currently three approaches in solving the problem:

(1) a purely empirical approach that was initially used by seismologists: determining the transfer functions of selected paths by processing a large body of data according to seasons, the time of day, and the type of weather,
(2) by adapting existing models of the atmosphere with due regard for winds at different heights, and
(3) by calculating the propagation conditions based on using current data of aerological sounding.

In this paper, we present the results derived from investigating a long path in the spirit of the last approach. We proceed from the assumption that a conventional method (the ray tracing method) allows us to reasonably well explain the propagation of the signal to distances of the order of 1500 km. The absorption (predominantly, nonlinear) along the path by far exceeding 1500 km is relatively large (Zarembo and Krasilnikov, 1966; Bass and Sutherland, 2004), because the signal "plunges" many times into the upper atmosphere, a region with strong absorption. In this case the large initial signal amplitude is unimportant. It is cut off at the first entry into the lower ionosphere.

Hence, in addition to the acoustic channel existing at the mesopause, an effective channel of propagation to large distances in the winter-time is provided by the acoustic channel in the tropopause and lower stratospheric region. Analysis of the conditions of signal propagation within the acoustic waveguide is based on using some integral indicator, the "AAC potential" (Ponomarev et al., 2006):

$$U = (\omega - k_x V_x)^2/c^2 - k_x^2, \tag{1}$$

where $\omega$ is the circular frequency of the sound wave, $k_x$ is horizontal wavenumber, $c$ is the velocity of sound, and $V_x$ is the wind velocity along the direction of wave propagation. The signal is transmitted when $U>0$. It is assumed that on the "wall" of the ACC (at the point of reflection) there is the node of the particle velocity in the wave and that the wind velocity is not large when compared with the velocity of sound. Then we obtain the quantization condition of the signal within the waveguide:

$$k_z H = \pi n \text{ or } k = \pi n/H \cos \Theta_n, \tag{2}$$

where $\Theta_n$ is the angle between the wave vector $\mathbf{k}$ and the vertical axis of the ACC, $H$ is the effective height, and $n$ is an integral number. Expressions (1) and (2) determine the quantization condition of the mode $n$ for the angle $\Theta$. From this it is easy to obtain the expression for the angle $\Theta_n$:

$$\Theta_n = \arccos[(\pi n/(H\sqrt{U}))\sqrt{\cos \Theta_0^2 - 2m \sin \Theta_0}]. \tag{3}$$

Here $m = V_x/c$, $n = 0,1,2,3\ldots$ is the number of the mode and $\Theta_0$ is the initial angle of the $n$th mode in the AAC. For instance, when $H = 6$ km, $m = 0.09$, $\lambda = 1.8$ km, and $\Theta_0 = 45^\circ$, in the ACC at a height of 12 km there can exist five modes: the zero mode propagating along the waveguide axis, the fundamental mode with $\Theta_1 = 80^\circ$, the second mode with $\Theta_2 = 70^\circ$, the third mode with $\Theta_3 = 54^\circ$, and the fourth mode with $\Theta_4 = 45^\circ$. The wind can change the angles drastically. For instance, for the mode with $n = 2$ (with the velocity of sound of about 306 m/s) an enhancement of the favorable wind by 20 m/s leads to an increase of the angle $\Theta_2$

by 10°, whereas the adverse wind of 50 m/s decreases $\Theta_2$ to a critical angle and, generally, destroys the waveguide channel. In the subsequent discussion, we shall examine the behavior of the sliding (zero) mode of the infrasound signal with $\omega = 1$ (the period $T \approx 6$ s) and its spatio-temporal structure at a maximum yearly temperature at a given height.

## 3. Use of the IDEAS meteorological data in developing the AAC model

When modeling the long-distance propagation of infrasound, it is important to know the structure of the AAC. The AAC structure is determined by the spatial distribution of meteorological parameters: temperature, and wind velocity and direction. Such data can be obtained using existing global models of the atmosphere, such as MSIS 2000. However, this model reproduces insufficiently accurately the spatial distribution of the wind field. Therefore, this paper uses archival data of aerological sounding of the atmosphere obtained under the Russia–USA IDEAS project. In this system, the aerological data are tied to the coordinate grid nodes and are interpolated along the longitude and latitude with a resolution of 2.5°, 5°, and 30°. The meteorological data are available virtually at any point on the terrestrial surface, including a gradation in height at the levels of 1000, 925, 850, 700, 600, 500, 400, 300, 250, 200, 150, 100, 70, 50, 30, 20, and 10 mb. Hence, each coordinate point in the IDEAS system has its own data file containing information on the time distribution of the necessary meteorological parameters (temperature, and wind velocity and direction) at 17 height levels, covering the time interval beginning in 1949. The IDEAS system provides 2.5°, 5°, or 30° spatial resolution. The number of available soundings is 4 times/day. The maximum height of probing reaches 10 mbar (about 36 km). The basic data were obtained using balloons. Details are provided by the site of the IDEAS system (Moscow and Bounder) (the IDEAS project servers: in Russia—http://teos1.wdcb.ru/esse, and in the USA—http://ideas.ngdc.noaa.gov), as well as, for instance, in a publication of Zhizhin and Andreyev (2004).

## 4. Assessing the state of the AAC for long-distance propagation of microbaroms

Many years of observations of microbaroms at the ISTP SB RAS Infrasonic Station indicate a characteristic seasonal variation with a maximum in the winter-time (Sorokin, 1995) characterizing both the transfer function of the AAC and the seasonal activity of the microbarom source, which, according to some data, coincides with the number of oceanic storms in the northern hemisphere (Tabulevich, 1981). An important result of the observations was the detection of two preferred directions in the arrival azimuths of microbaroms: to the North Atlantic with an azimuth of about 320° and to the Northwestern Pacific with an azimuth of 60° (Fig. 1). This suggests a need to construct the AAC model for two paths (Fig. 2) and compare it with experimental data. Our study considers the properties of long-distance propagation of microbaroms, or known as infrasonic waves, from storm features in seas and oceans that are the most active in the winter-time in the North Atlantic. Microbaroms were used to test the AAC for several reasons: firstly, these signals are highly capable of propagating to long distances and, secondly, the microbaroms have a counterpart or an ''antipode'' that does not experience any atmospheric variations and that can be used to infer temporal changes in the ACC. They are microseisms. Besides, when observing microbaroms, we carry out substantial filtering of infrasonic signals from the other types, including atmospheric noise. Moreover, using the procedure of calculating the AAC potential, we analyzed only one selected direction to the source. For the North Atlantic this direction is 320°. In our opinion, the proportional of infrasonic signals (not microbaroms) generated in the auroral zone and entering into the AAC along this direction is not significant.

The time interval under examination spans the year 1986 for 17 selected coordinate points along the North Atlantic—Beijing path, and for 15 points

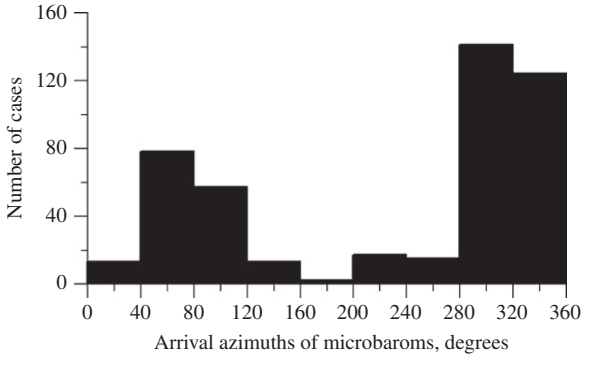


Fig. 1. Predominant arrival directions of microbaroms at station ''Badary'' (Irkutsk).

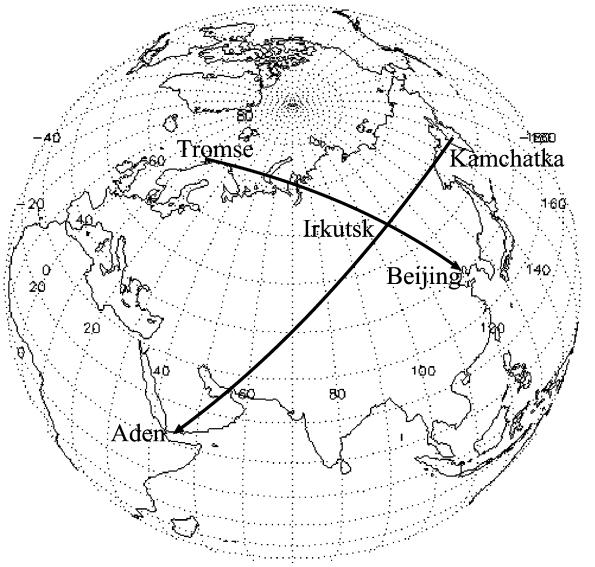


Fig. 2. Two possible acoustic paths of microbarom propagation.

along the Kamchatka—Aden path. These paths are Northeastern Atlantic-oriented with an azimuth of about 320° and Northwestern Pacific-oriented with an azimuth of 60° relative to the receiver at Irkutsk, which corresponds to the preferred arrival azimuths of microbaroms at ISTP SB RAS Infrasonic Station "Badary".

## 5. AAC modeling results for long-distance propagation of microbaroms

### *5.1. Spatio-temporal distribution of the AAC potential*

Before proceeding to the description of the results of calculations of these paths, we will first point to some important limitations used in this study. In the first place, the source position is considered fixed when calculating the propagation conditions of infrasound signals along the path. Secondly, our calculations neglect the influence of the vertical wind components. Indeed, the proportion of the vertical wind constitutes only 5–7% of the zonal wind.

Figs. 3 and 4 present the results from calculating the potential $U$ of the acoustic channel for some characteristic points along the paths under investigation. The figures portray the height profile of the annual variation of the potential $U$. The potential $U<0$ appears totally black, showing the blanking (no-propagation) zone, and $U>0$ appears light, showing the signal propagation (channeling) zones. The axis of ordinates indicates the isobaric heights (millibars, with the geometrical height increasing downward), and the abscissa axis indicates time in units of meteorological probe launchings (4 times/day, totaling 1460 counts in a year). Thus the values of the potential $U$ have the form of height profiles of the annual variation of the acoustic signal channeling zones for the aforementioned points. Common to the points along the AAC path from the Atlantic are some distinctive features, namely, in the summer the potential $U$ has minimum values (appearing black). The regional characteristics of the AAC are also presented in Figs. 3 and 4. It is seen that the AAC in China and East Siberia is generated mostly in the winter-time at 200–300 mb heights (9–12 km), with a tendency for the height of the AAC axis to increase westward (Fig. 3a and b). Furthermore, the figures clearly show an oscillatory structure with a period of 10–15 days, which is likely caused by synoptic phenomena. In West Siberia (Fig. 3c and d), the height position of the AAC axis increases to about 20–50 mb (25–29 km). A tendency for the AAC height to increase is also observed in the area of the North Atlantic (Murmansk and Tromse, Fig. 3e and f). This suggests that the state and position of the AAC along the North Atlantic–China path in the winter-time is determined by westerly winds coinciding with the direction from the source to the receiver.

Let us now consider the conditions of AAC generation for the source lying eastward of the receiver at Irkutsk (the Kamchatka–Aden path). Fig. 4a–f, plotting the height profiles of the AAC potential along the path, shows a seasonal variation with a maximum in the winter, except in equatorial areas (Fig. 4e and f). A periodic structure of a synoptic character is also distinguished. Here, the functioning of the AAC has a short-lasting, sporadic character. This seems to be due to the fact that the prevailing westward zonal transfer changes eastward at some instants of time to produce the waveguide.

As the equator is approached, the waveguide conditions are impaired, and at some points the AAC disappears altogether (Urumchi, Fig. 4d). In the equatorial regions (Kandagar and Aden), the AAC activity is enhanced abruptly (Fig. 4e and f). Contrary to the state of the AAC in mid-latitudes, the maximum of seasonal variation here corresponds to the summer season. Most likely this is due

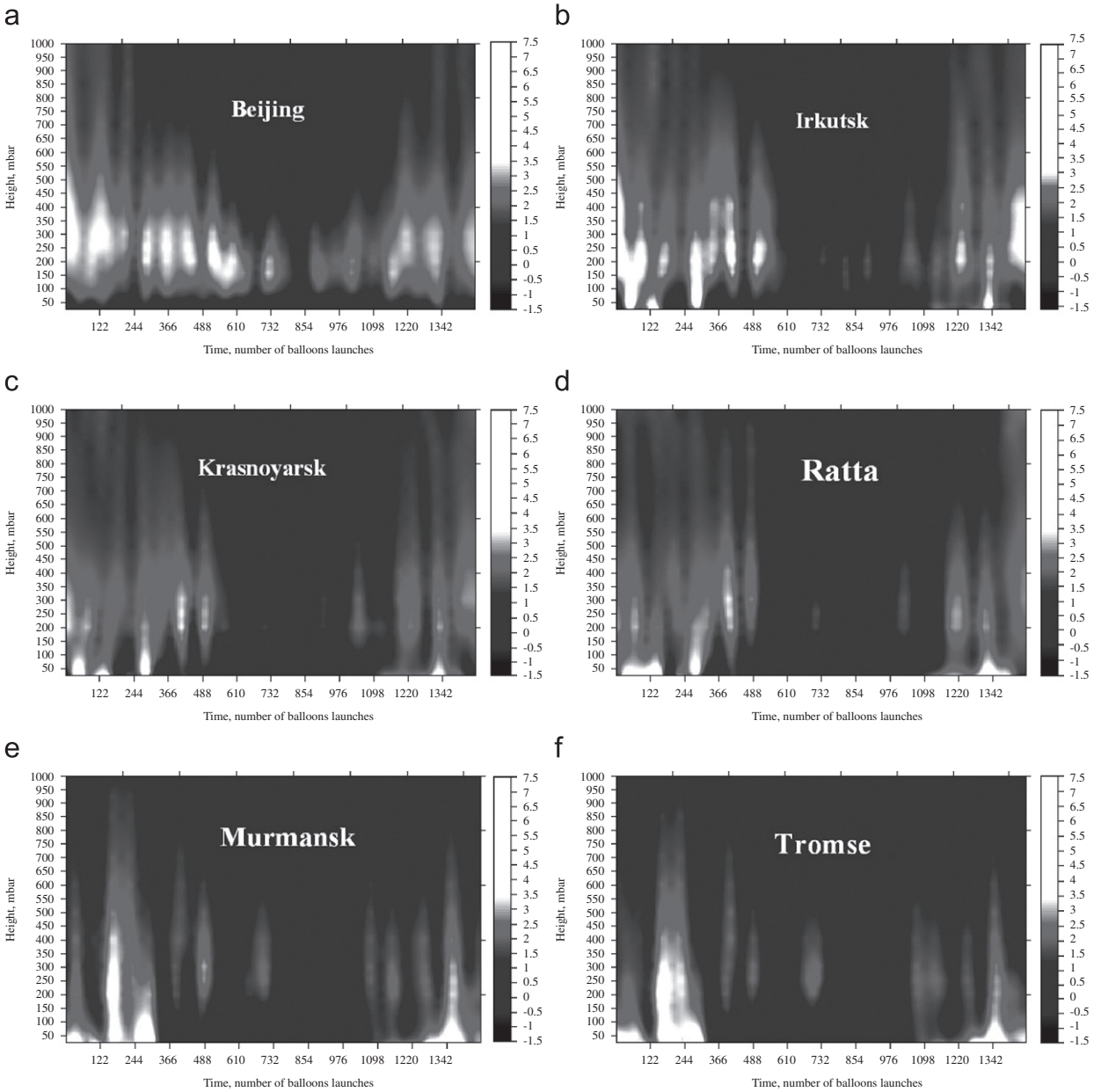


Fig. 3. Spatio-temporal structure of the potential $U$ of the atmospheric acoustic channel for the North Atlantic (Tromse)–Beijing path.

to the existence of an equatorial jet flow at heights of 25–30 km at these latitudes in the summer-time (Vorobyev, 1991). At this stage we will not consider in detail the influence of the equatorial jet flow on the AAC generation.

According to our data, the North Atlantic source of microbaroms is more active than the Pacific source. Fig. 1 reflects this. We see not only the predominant action of the Atlantic source but also the fact of predominant action of the atmospheric circulation favoring the propagation of signals from the Atlantic eastward. The situation with the direction to the Pacific source is different. Here, operation of the AAC has the short-lasting, occasional character caused by sporadic easterly winds. In this paper we did not intend to make a detailed study of the state of the AAC depending on meteorological parameters at each point.

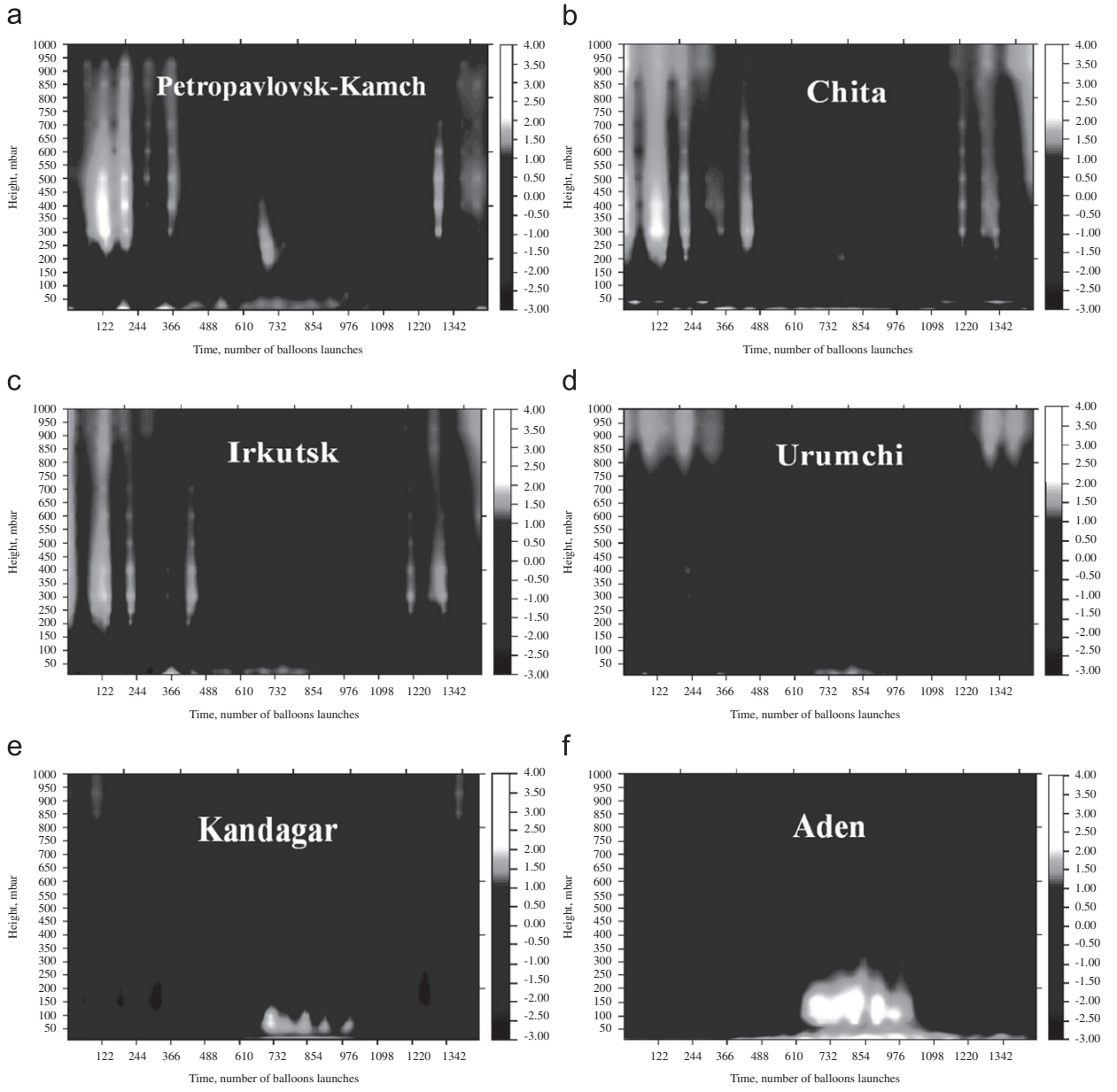


Fig. 4. Spatio-temporal structure of the $U$ potential of the atmospheric acoustic channel for the Kamchatka–North Africa (Aden) path.

### 5.2. Modeling of the structural AAC parameters

As regards the signal propagation within the AAC, of interest is the behavior of the AAC boundaries, and of the upper boundary (blanking zone A) in particular, where $U<0$, because this zone is in essence a potential barrier for acoustic energy escaping to the upper atmosphere. The effectiveness of such a barrier can be estimated by integrating the potential $U$ of the acoustic channel from the height $h_1$ to $h_2$:

$$I_A = \exp(A), \text{ where } A = \int_{h1}^{h2} \sqrt{|U|}\,\mathrm{d}h, \tag{4}$$

and assuming that the acoustic energy attenuates exponentially, as the AAC potential $U<0$. We do not consider here the height region above 100 km, where $U$ is also negative. Fig. 5a and b plots the potential $U$ for the winter conditions (curve 1), and for the summer conditions (curve 2) calculated,

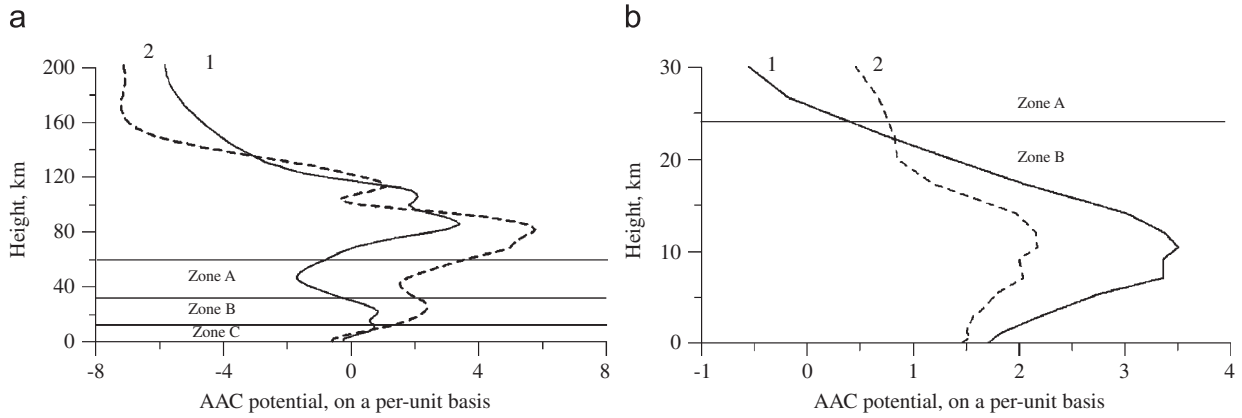


Fig. 5. The blanking zones as calculated from the MSIS 2000 model for 10 January 1986 (curve 1) and for 25 July 1986 (curve 2) for the source in the Atlantic (a); the same, but for the IDEAS data (b).

respectively, in the MSIS 2000 model (a) and from the IDEAS data (b) Irkutsk for the North Atlantic source. Further, the signal "blanking" within the waveguide is considered effective, if signal leakage through the blanking layer is no more than 0.1 of the value of the signal.

It is evident from Fig. 5a that the AAC potential for the winter and summer has fundamental differences, namely, two zones with $U<0$ are distinguished: blanking zone A at heights between 30 and 50 km, and blanking zone C in the ground layer at heights between 0 and 4 km (Fig. 5a, curve 1). Zone B corresponds to the AAC. In the summer (Fig. 5a, curve 2), the AAC potential is distributed in the height in such a manner that there is only blanking zone C, whereas upper blanking zone A is absent altogether. Thus the model calculations of the AAC potential for the winter and summer show that in the winter the AAC potential produces a highly effective channeling zone bounded by two blanking layers, whereas in the summer, because of there being no blanking layer A, acoustic energy escapes to the upper atmosphere and is absorbed there.

We now turn our attention to the potential $U$ calculated using the IDEAS data. It should be noted that the height profile of the potential $U$ is not necessarily negative (even in the winter), i.e. it produces a blanking layer and, therefore, the effectiveness of this layer was estimated only for the cases where $U$ changes sign.

Fig. 5b plots the profiles of the AAC potential for the winter and summer, calculated from the IDEAS data. It is seen that an effective blanking layer is observed in the winter at heights between 24 and 30 km (Fig. 5b, curve 1). Furthermore, the blanking layer is not manifest in the ground layer, whereas neither the upper blanking layer nor the ground blanking layer is observed in the summer-time (Fig. 5b, curve 2). Hence, the IDEAS data, like the MSIS 2000 model, confirms the existence of an effective blanking layer several kilometers in thickness in the winter-time.

The possible reason behind the appearance of the blanketing zone C in these two figures could be the appearance of a temperature inversion or the variations of the zonal wind coinciding in direction with the signal propagation. The winter-time is dominated by the westerly wind (from the west), and the summer-time is dominated largely by the easterly wind (from the east). Since the temperature inversion is not observed in either case, the production of zone C can be associated with the favorable wind direction for this case. Here, the production of zone C is associated with the appearance of the oppositely directed wind to the signal propagation at this height level (4–5 km). Besides, one further reason for the differences in the description of the AAC potential would also reside in imperfection of the model for wind field variations.

It is worth noting that the IDEAS data cover the height range below 30 km, and, as is apparent from Fig. 5a (curve 2), the AAC potential above 30 km is also negative. Therefore, our estimate of the effectiveness of the blanking layer is only minimal rather than a complete one; nevertheless, it testifies that the acoustic channel is generated. The effectiveness of this layer in January 1986 for station Badary was calculated according to Eq. (4) and is plotted in Fig. 6, where the axis of ordinates

indicates the effectiveness of signal blanking with height on a logarithmic scale, and the abscissa axis indicates the current time of January 1986 in days. It is seen that the blanking layer was observed in January 1986 for more than 15 days, and the blanking effectiveness of the layer was larger by about a factor of 10–100. Such an attenuation of the signal corresponds to the 6-km atmospheric layer in the height range from 24 to 30 km, where $U<0$.

The height position of the blanking layer can be estimated by assuming that on the boundary of this layer there is a tenfold attenuation of the signal by this layer, according to Eq. (4). Fig. 7a (solid curve) plots the height position of the blanking layer boundary, which, according to the IDEAS data, persisted in January 1986 for 15 days at heights below 30 km. This period corresponded to an effective functioning of the AAC. Further, an abrupt expansion of the ACC occurred after 15 January 1986, followed by its total disappearance. Dashes show the continuation of the layer height for the case of a linear decrease in AAC potential above 30 km (as in the MSIS model). The number of possible modes of the propagating infrasound signal, trapped within the acoustic channel, at the initial angle of 45° for January 1986 is presented in Fig. 7b.

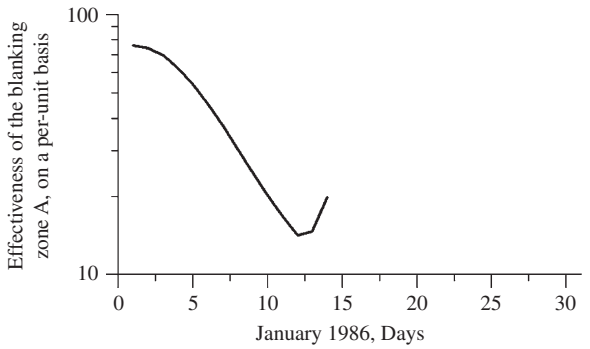


Fig. 6. Effectiveness of the blanking 6-km layer at station "Badary" for the Atlantic–Beijing path, January 1986.

The effect of the operating acoustic channel is illustrated in Fig. 8 for long-distance propagation of microbaroms as observed at ISTP SB RAS Infrasonic Station Badary, Irkutsk (51.45N, 102.13E) in the first half of January 1986. In this figure, the axis of ordinates indicates the arrival azimuths of microbaroms, and the abscissa axis indicates hours/days of recording infrasound signals from 1 January to 14 March 1986. In the second half of January 1986, the blanking layer at 24–30 km disappeared; accordingly, the conditions of AAC existence were disturbed. On the other hand, the infrasound signal with an azimuth of ~320° ceased to arrive at Infrasonic Station Badary (Irkutsk); instead, the signal with an azimuth of about 60° appeared.

Let us consider the state of the AAC for infrasound signals arriving at station Badary from the Northwestern part of the Pacific, with an azimuth of about 60°. Looking at the observational data on microbaroms, we see that the state of the AAC from this direction can be characterized as sporadic or having an occasional character. However, let us consider this phenomenon consistently in terms of the atmospheric MSIS 2000 model and using the IDEAS data. The AAC potential,

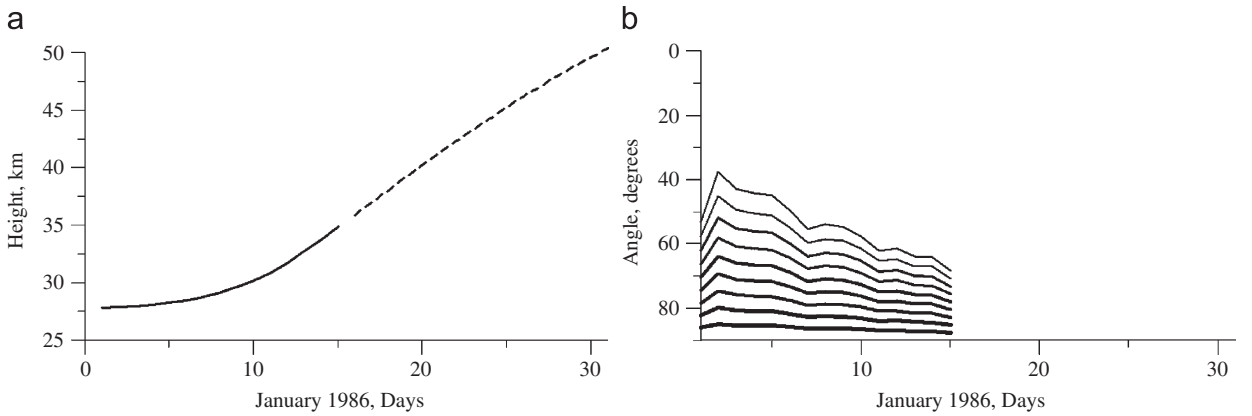


Fig. 7. The height of the blanking layer as calculated from the IDEAS data for January 1986 (the dashed line shows the continuation of the layer's height, for the case of a linear decrease in potential $U$ above 30 km (as in MSIS 2000) (a), and the number of propagating modes corresponding to a given width of the atmospheric acoustic channel (b).

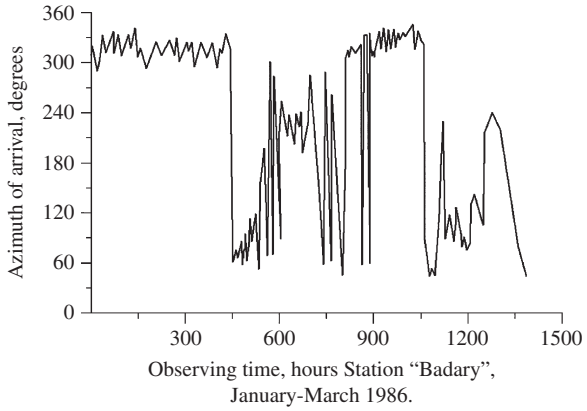


Fig. 8. Arrival azimuths of microbaroms at ISTP SB RAS Infrasonic Station "Badary" in 1986 (Sorokin, 1995).

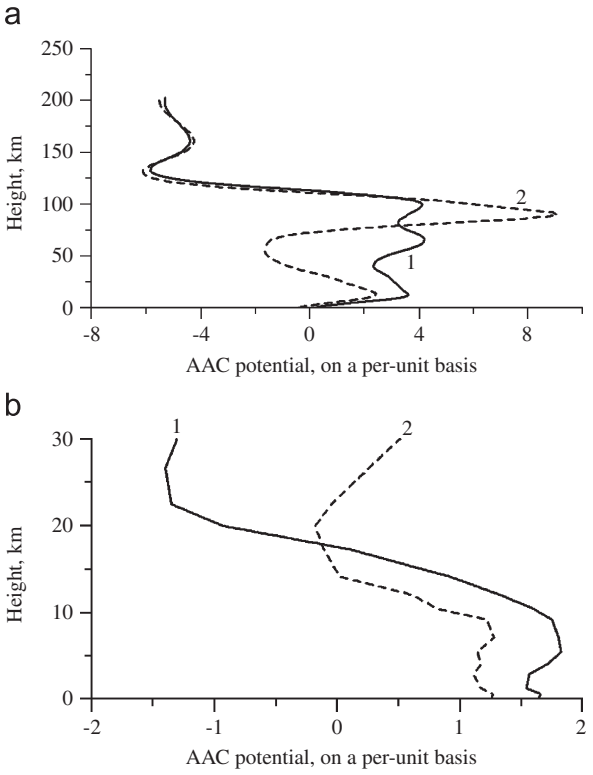


Fig. 9. (a) AAC potential for the source in the Pacific in the winter on 10 January 1986 (1) and in the summer on 25 July 1986 (2) from the MSIS 2000 data. (b) AAC potential for the source in the Pacific in the winter on 10 January 1986 (1), and in the summer on 25 July 1986 (2) from the IDEAS data.

calculated in the MSIS model and plotted in Fig. 9a (curve 1), shows that in the winter (for example, for 10 January 1986), no acoustic channel must be present, because $U>0$ holds all the time. This is consistent with the universally accepted view of the zonal circulation at the tropopause height where in the winter the wind has a preferred westerly (from the west) direction, i.e. opposite to the direction of signal propagation. In the summer (Fig. 9a, curve 2), similar calculations of the AAC potential give regions where $U<0$, i.e. there are blanking regions for the infrasound signal and, hence, the conditions for waveguide propagation.

Calculations using the IDEAS data give contrary results. More specifically, the plot of the AAC potential (Fig. 9b, curve 1) for 10 January 1986 suggests the presence of a waveguide AAC, whereas in the summer the effective AAC is not always present: for instance, while in early July 1986 there is a sufficiently effective blanking layer, it disappears altogether at the end of July 1986 (Fig. 11a). Our subsequent discussion will be based on the AAC properties calculated from the IDEAS data, and from observational evidence.

We believe that the data from IDEAS must more adequately correspond to atmospheric parameters than does the MSIS model. Indeed, in the winter-time the AAC potential, calculated from the IDEAS data, undergoes first some decrease with the height and then a considerable increase associated with an enhancement of the favorable wind to a height of about 10 km; at higher altitudes the wind begins to vary in intensity and, more importantly, in its directions. At the height of about 20 km there appear transverse and oppositely directed wind components producing a blanketing zone of type A. This is not observed in the summer-time. However, calculations in the MSIS model provide results on the propagation in the AAC in agreement with experiment (in winter, the AAC from the Pacific is often blanketed). Thus, in our view, this difference, when the potential is calculated, is due to the fact that the MSIS model uses averaged data, whereas in the IDEAS data we use only a portion of the winter situation.

If we compare the AAC effectiveness from the North Atlantic with the AAC effectiveness from the Northwestern Pacific, the number of strong storms occurring on these water surfaces is the most striking feature. It is seen that the AAC from the Pacific is effective in the winter, but it is less effective than the acoustic channel from the North Atlantic; moreover, the number of active storms in the Atlantic is larger than that in the Pacific. We identify the possible variations in the source with the data on the number of storm features separately for the Atlantic and the Pacific for 1986.

Table 1
Monthly number of storms in the North Atlantic and in the Pacific for 1986, and their total values (Tabulevich, 1995)

| Region | Month | | | | | | | | | | | | |
|---|---|---|---|---|---|---|---|---|---|---|---|---|---|
| | J | F | M | A | M | J | J | A | S | O | N | D | Sum |
| Atlantic | 18 | 04 | 18 | 06 | 04 | 05 | 04 | 09 | 14 | 20 | 14 | 19 | 135 |
| Pacific | 14 | 11 | 10 | 04 | 03 | 00 | 00 | 04 | 02 | 12 | 13 | 11 | 84 |

The corresponding data on the total number of storms in the Atlantic and in the Pacific for the period being analyzed are taken from a paper of Tabulevich (1995) and are listed in Table 1. This is of significant importance interpreting the number of received signals from the North Atlantic, and from the Pacific (Fig. 1).

In the summer season, the ACC from the Atlantic is totally blanked, which is supported by calculations in the MSIS model and from the IDEAS data, as well as by microbarom observations (Sorokin, 1995); furthermore, the number of active storms is significantly smaller when compared with the winter season. Therefore, almost no microbaroms from the Atlantic are observed at this period. On the contrary, the AAC from the Pacific is open sporadically in the summer season but, generally, during a sufficiently long time interval, so that the occurrence of microbaroms can be detected. Besides, the number of active storms in the Pacific is also small in the summer season. Accordingly, the number of infrasound signals received from the Northeastern Pacific is also small at that period.

There are strong grounds for believing that in the winter the AAC from the eastward direction does exist. This is supported by calculations using the IDEAS data as well as by the observational data from Infrasonic Station Badary for the year 1986. Calculations of the height position of the boundaries for January and July 1986 were performed from the IDEAS data; the results are presented in Figs. 10a and 11a. It is seen that the AAC for January 1986 has a larger effective width than in July 1986 and, hence, has a larger modal capacity. Calculations show further that the AAC from the eastward direction does persist, at least, throughout January 1986.

The calculation results plotted in Fig. 9b (curve 2) and Fig. 11a show that the AAC from the eastward direction exists also in the summer, but with lower effectiveness. The height position of the AAC boundary changes from 13 km in early July 1986

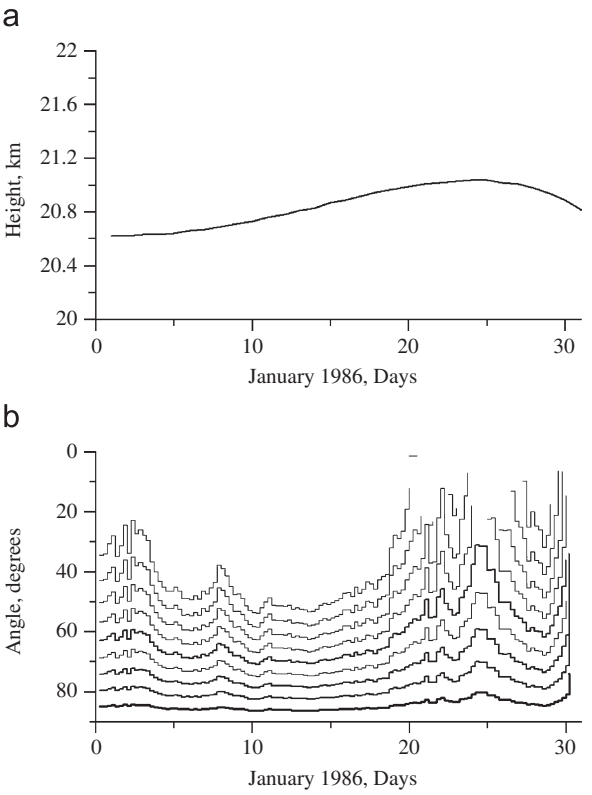


Fig. 10. (a) Pacific, AAC boundaries, January 1986. (b) Pacific, number of modes, January 1986.

to 26.5 km on 27 July 1986, followed by a total disappearance of the channel.

The number of propagating modes in the acoustic channels from the Atlantic and from the Pacific, corresponding to January and July 1986, is presented in Figs. 7b, 10b, and 11b. It is evident that in the winter the AAC from the North Atlantic is more intense than in the summer, which is ensured by the wind direction. The effective width of the ACC from the Atlantic is less intense but sufficiently effective in the winter season—more than nine modes can also be excited in it from time to time. The ACC from the Pacific is less effective in July 1986—about six modes can be observed in this case.

We shall now highlight the correspondence of the number of observed and calculated wave modes for January 1986. Calculations using the IDEAS data give about nine propagating modes along the path from the Atlantic (Fig. 7b). In point of fact, the recorded angular spectrum of the arrival of microbaroms for 11–12 January 1986 shows that only about five modes are observed (Fig. 12). It can also be seen that there is a considerable broadening of

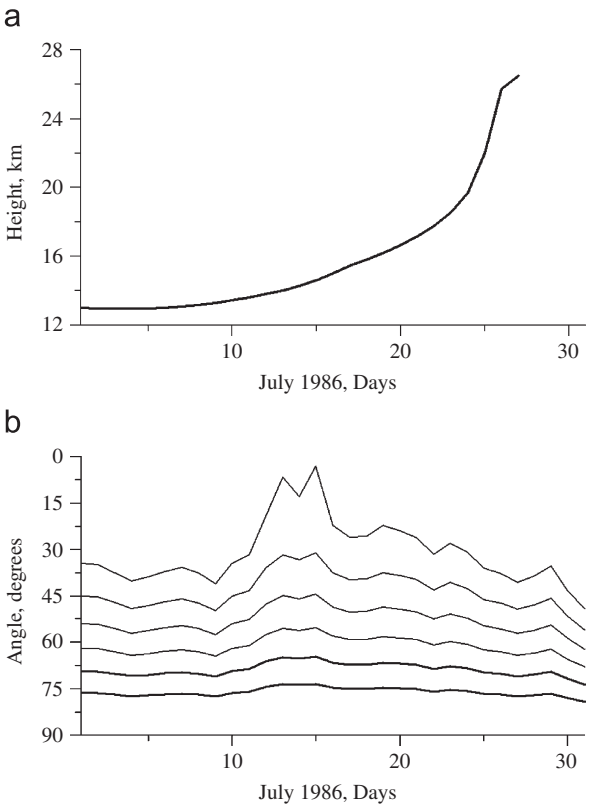


Fig. 11. (a) Pacific, AAC boundaries, July 1986. (b) Pacific, number of modes, July 1986.

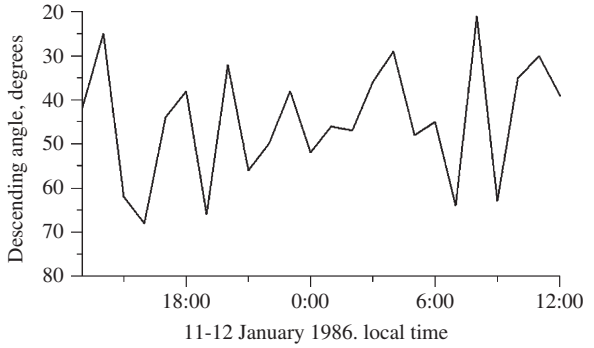


Fig. 12. Vertical arrival angle of microbaroms on 11–12 January 1986, station "Badary" (Irkutsk).

the angular spectrum during the daytime when compared with the night-time. Such variations of the angular spectrum or modal composition of the ACC can be accounted for by the enhancement of the wind flow associated with solar radiation.

The connection of the wind regime in the upper atmosphere with the received infrasound waves would seem obvious. In actual fact, the wind directions and azimuths are interlinked in a rather complicated way. It turned out that the wind direction at Irkutsk for the winter–spring 1986 period behaves in concord with the received signals only at definite heights, namely, at 5.5–12 km. The best agreement between the wind direction for January–March 1986 and the variations of the arrival azimuths of microbaroms corresponds to a height of 400 mb (7.7 km). There is a time coincidence of the unperturbed portion with the period of greatest perturbation of the angles of arrival of microbaroms and of wind direction. The study of the properties of the effects of the wind regime at different heights on the conditions of microbarom propagation and their participation in the subsequent propagation is beyond the scope of this paper.

## 6. Conclusions

The results of this study may be summarized as follows:

1. We have suggested the technique for calculating the AAC, based on using the archived data from IDEAS and observations of long-distance infrasound propagation.
2. The AAC was examined for two preferred arrival directions of microbaroms from the Atlantic (azimuth $\sim 320^\circ$) and the Pacific (azimuth $\sim 60^\circ$) to station Badary (Irkutsk).
3. The height profiles of the AAC model potential $U$ were compared with the potential calculated from the meteorological IDEAS data for the winter and summer propagation conditions. The comparison showed some difference in the location of the blanketing layer calculated on the basis of IDEAS and MSIS, where the signal is attenuated by a factor of 10; respectively, it is 26 and 34.5 km. It was found that the IDEAS data show that in the winter-time, an effective acoustic channel is located in the area over Irkutsk at tropopause and lower stratospheric heights of up to 26 km.
4. An estimate was made of the effectiveness of the blanketing layer 6 km in height for the winter-time conditions along the North Atlantic–Beijing path. It was found that when the signal is transmitted by the blanketing layer, it is attenuated by a factor of about 100. This layer persists for about 15 days and lies at heights from 26 to 35 km. It indicates the existence of an effective AAC in the area over the infrasonic Badary station.

5. The study demonstrated the spatio-temporal structure of the AAC for some of the points along the paths. For instance, for the Beijing point the axes of the acoustic channel lie at a height of 200–250 mbar (10–15 km).
6. The differences in the winter and summer modal composition of the ACC and its generation mechanism were shown.

## Acknowledgment

We are grateful to Mr. V.G. Mikhalkovsky for his assistance in preparing the English version of this paper.

## References

Bass, H.E., Sutherland, L.C., 2004. Atmospheric absorption in the atmosphere up to 160 km. Journal of the Acoustical Society of America 115, 1012–1032.

Blanc, E., 2001. Infrasons Propagation Reseau IDC Bruit de Fond et Infrasons d'Origine Naturelle. Comissariat a l'Energie Atomique. Laboratoire de Detection et de Geophysique. B.P., Bruyeres-le-Chatel, p. 72.

Drob, D.P., 2003. Detailed specification of the atmosphere for infrasound propagation modeling. SRR 2003. In: Proceedings of the 25th Seismic Research Review—Nuclear Explosion Monitoring: Building and Knowledge Base, September 23–25, 2003, Tucson, AZ 〈https://www.nemre.nnsa.doe.gov/prod/researchreview/2003/papers/07-04.pdf〉.

Drob, D.P., Picone, J.M., Garces, M., 2003. The global morphology of infrasound propagation. Journal of Geophysical Research 108 (D21), 4680.

Gibson, R.G., Drob, D.P., 2005. Infrasound propagation calculation techniques using synoptic and mesoscale atmospheric specifications. In: 27th Seismic Research Reviews: Ground-Based Nuclear Monitoring Technologies, Rancho Mirage, CA, September 20–22, 2005 〈https://www.nemre.nnsa.doe.gov/prod/researchreview/2005/PAPERS/06-02.PDF〉.

Liszka, L., 1974. Long distance propagation of infrasound from artificial sources. Journal of the Acoustical Society of America 56, 1383–1388.

Massey, H.S.W., Boyd, R.L.F., 1957. The Upper Atmosphere, New York.

Massey, H.S.W., Boyd, R.L.F., 1962. The Upper Atmosphere. Gudrometeoizdat, Leningrad, 376pp. (Russian translation).

Ponomarev, E.A., Rudenko, G.V., Sorokin, A.G., Dmitrienko, I.S., Lobycheva, I.Yu., Baryshnikov, A.K., 2006. Using the normal-mode method of probing the infrasonic propagation for purposes of the comprehensive nuclear-test-ban treaty. Journal of Atmospheric and Solar-Terrestrial Physics 68, 599–614.

Sorokin, A.G., 1995. The study of long-distance infrasound propagation from explosions and oceanic storms. Candidate of Science (Physics and Mathematics) Dissertation, Irkutsk, 115pp.

Tabulevich, V.N., 1981. Comprehensive Investigations Into Microseismic Vibrations. Nauka, Novosibirsk, 151pp.

Tabulevich, V.N., 1995. On recordings of global microseismic vibrations and observations of microseisms in shore zones of oceans. Physics of the Earth and Planetary Interiors 91, 299–305.

Vorobyev, V.I., 1991. Synoptic Meteorology. Gidrometeoizdat, Leningrad, 616pp.

Zarembo, L.K., Krasilnikov, V.A., 1966. An Introduction to Nonlinear Acoustics. Nauka, Moscow, 520pp.

Zhizhin, M.N., Andreyev, A.V., 2004. Network services on solar–terrestrial physics, meteorology, geodynamics, and seismology in the GRID standard for the "Electronic Earth" RAS Program. In: International Conference IKIR DVO RAN. Petropavlovsk-Kamchatsky, 14–21 August 2004. Collection of papers, p. 11.